THREE-DIMENSIONAL IMAGING WITH LARGE-AREA POSITRON CAMERAS

V. Perez-Mendez, L.T. Chang, J.P. Lenahan, and B. Macdonald

Lawrence Berkeley Laboratory
University of California
Berkeley, California

ABSTRACT

Cameras for nuclear medicine imaging which use the two back-to-back gamma rays from a positron annihilation have the unique property of being able to give images of positron-emitting radionuclide distributions without the use of collimators and the associated large loss of intensity. Cameras with two parallel opposing planar gamma-ray detectors are now commonly used without camera movement to give tomographic images of a number of transverse planes through the positron emitting object. Each of these tomographic images, the set of intersections of the decay-gamma event lines with that plane, has source points in that plane in focus but superimposed on a large background from the blurred-out images from the other planes.

We present here a method of three dimensional image reconstruction of these positron images which uses a single exposure to remove the blurred off-plane activity from all tomographic planes simultaneously. The tomographic image on a plane is the sum of contributions from all source planes, each contribution being the convolution of the source distribution on a plane with the camera system point response function for that plane. Fourier transformation of the set of tomographic image equations gives a set of linear equations whose solution, after inverse Fourier transformation, are the desired source reconstructions.

INTRODUCTION

Nuclear Medicine cameras using the pinhole or the parallel-hole collimator determine the direction of a gamma-ray emitted from a point in a radionuclide distribution. An image produced by these cameras is a projection of the object and contains no depth information because a given object point is imaged from only a single direction. The positron camera also determines only the direction taken by the two 511 KeV annihilation gamma-rays from a positron event but it views each source point from a range of angles and images produced by this camera contain depth information about the object.

The large-area type of positron camera considered here (Fig. 1) produces images of a volume distribution of radionuclides[1-3] while the ring camera generally images a two-dimensional slice of the distribution. Images from these large-area cameras have generally been tomographic images. These are produced when the set of positron events are projected onto transverse planes through the object. From Fig. 1 one can see that these tomographic images have those sources on a given plane in focus while all other planes contribute a blurred background superimposed on the in-focus information. The method of three-dimensional imaging we describe below removes this background simultaneously from a number of these tomographic images from the positron camera. It requires a knowledge of the geometric imaging properties of the camera, contained in the point response functions, and obtains reconstructions of the original object on these planes using a Fourier transform, matrix inversion,

technique.

The data required for this 3-D image reconstruction method is taken in one exposure and does not require a rotation of the camera about the object. Image reconstruction has been done with large-area positron cameras with the techniques of Computerized Tomography together with camera rotation[4] but this latter method uses the positron data quite inefficiently. Because the method described here takes projections of an object from a restricted range of angles instead of the full 180^{o} used in Computerized Tomography the image reconstructions, as will be seen, do not reproduce the very lowest spatial frequencies of the object.

The method is applicable to a number of other existing cameras which also produce tomographic images, such as the rotating slanted-hole collimator camera.[5] With a similar method, also using tomograms but subtracting only an approximate background from the nearest neighbor plane, Myers has made reconstructions with the Anger tomographic scanner.[6]

IMAGE RECONSTRUCTIONS FROM TOMOGRAMS

We express the three dimensional object by its values $o_i(\underline{r})$, $i = 1,...N$, on N adjacent planes separated by the depth resolution of the positron camera. Tomographic images $t_j(\underline{r})$ are formed on each of these planes by projecting through a given plane, for each positron event, the line connecting the measured points of intersection of the two positron gamma-rays (Fig. 1) with the camera's two planar detectors. An examination of the equations which relate the functional dependence

of $t_j(\underline{r})$ on the object distributions $o_i(\underline{r})$ will show how to solve for the o_j's.

To obtain these equations we use the point response functions $h_{ij}(\underline{r},\underline{r}')$, i,j = 1,...N, which are the measured response of tomographic plane j at $\underline{r}$ to a single point source of unit intensity located at $\underline{r}'$ in plane i. The point response functions for a three-plane system are pictured in Fig. 2. Measured point response functions for the University of California, San Francisco, (UCSF) positron camera are given in Fig. 3. The functions shown have used only those positron events for which $|x_2 - x_1| \leq d$ and $|y_2 - y_1| \leq d$ where d is somewhat smaller than the full width of the square detectors used. When this is done the point response functions depend only on the difference $\underline{r} - \underline{r}'$ and they remain constant in shape, size, and intensity as the point source moves in a given plane over the camera field of view for that plane. This region of constant detection efficiency (spatial invariance) is, for the mid-plane, a square of width W - d. We have used this condition of spatial invariance to make possible a direct solution for the object distributions $o_i(\underline{r})$ without requiring iterative procedures.

Since $h_{ij}(\underline{r}-\underline{r}')$ represents the response of a tomographic plane j to a unit point source at $\underline{r}'$ on plane i, the response to $o_i(\underline{r}')$ is just $o_i(\underline{r}')\, h_{ij}(\underline{r}-\underline{r}')$ and the response to the entire plane i is $\int o_i(\underline{r}')\, h_{ij}(\underline{r}-\underline{r}')\, d^2\underline{r}'$. Since all planes i = 1,...N contribute to tomographic plane j we can write

$$t_j(\underline{r}) = \sum_{i=1}^{N} \int o_i(\underline{r}')\, h_{ij}(\underline{r} - \underline{r}')\, d^2\underline{r}' \qquad j = 1,...N \qquad (1)$$

This is the well-known convolution integral which we can write as

$$t_j(\underline{r}) = \sum_{i=1}^{N} o_i(\underline{r}) * h_{ij}(\underline{r}) \qquad J = 1,\ldots N \qquad (2)$$

The Fourier transform, which transforms the spatial functions $t_j(\underline{r})$, $o_i(\underline{r})$, $h_{ij}(\underline{r})$, to functions of spatial frequency $T_j(\underline{u})$, $O_i(\underline{u})$, $H_{ij}(\underline{u})$, has the unique property, for real and complex functions, that the transform of the convolution integral is equal to the product of the transforms of the two functions o_i and h_{ij}. Thus, we can take the Fourier transform of both sides of Eq. 2 to give a set of linear equations in the transform quantities.

$$T_j(\underline{u}) = \sum_{i=1}^{N} O_i(\underline{u})\, H_{ij}(\underline{u}) \qquad j = 1,\ldots N \qquad (3)$$

For all spatial frequencies for which the determinant $D(\underline{u}) = |H_{ij}(\underline{u})|$ is not zero we can solve for $O(\underline{u})$ using the inverse matrices $H_{jk}^{-1}(\underline{u})$.

$$O_k(\underline{u}) = \sum_{j=1}^{N} T_j(\underline{u})\, H_{jk}^{-1}(\underline{u}) \qquad k = 1,\ldots N \qquad (4)$$

An inverse Fourier transform of the function $O_k(\underline{u})$ determined by this equation gives the required object plane distributions $o_k(\underline{r})$. Note that the positron camera data for the object is contained in the quantities $T_j(\underline{u})$ and that the inverse matrices $H_{jk}^{-1}(\underline{u})$ depend on the camera point responses and the number and separations of the tomographic planes. The solution of Eq. (3) requires the inversion of an N x N matrix for each value of $\underline{u}$, 4096 times if the tomographic planes are digitized on a raster of 64 x 64 bins. Since N is a fairly small number, on the order of 5 to 10, this presents no computation problems. Once the inverse matrices are calculated and stored, for instance, on the magnetic disk of a small computer, object plane solutions $O_k(\underline{u})$ are easily calculated as linear combinations of the tomographic data $T_j(\underline{u})$.

RESPONSE TO LOW SPATIAL FREQUENCIES

When the determinant $D(\underline{u})$ is zero at a given spatial frequency $\underline{u}$ then $O_i(\underline{u})$ cannot be determined for any plane. The general form of $D(\underline{u})$ for positron cameras is that it is zero at $\underline{u} = 0$ with a small slope near zero but with a rapid increase with increasing $\underline{u}$ to its maximum value. Experience has shown that for the point response functions encountered with positron cameras the only zero of $D(\underline{u})$ is at $\underline{u} = 0$.

Since the zero spatial frequency function is a constant as a function of $\underline{r}$, the solutions $o_i(\underline{r})$ obtained with this method are indefinite by an additive amount. This constant for each plane must be determined by some subsidiary condition, for instance, that $o_i(\underline{r})$ has no negative values. This has been done in Fig. 4 for tomograms produced in a computer simulation of a positron camera in the limit of a large number of events, with excellent agreement of the reconstructions with the original object planes.

The effect of statistical variation in the tomograms on the reconstruction is of critical importance and we have investigated this using a Monte Carlo simulation with a PDP 11/45 computer. The system modelled used two square detectors, 64 cm on a side and separated by 64 cm, to image a positron-emitting object in the shape of an octahedron (Fig. 5). To facilitate future comparison with a seven plane reconstruction, Fig. 6 shows what one would expect to see on each of seven planes when only the octahedron activity in the volume immediately surrounding each of the planes $t_1, t_2, \ldots t_7$ of Fig. 5 is considered.

About two million positron events were generated, 50 events from each of the inner bins of the octahedron and 200 from the outer bins,

uniformly distributed in solid angle between $\theta = -26^{o}$ and $\theta = +26^{o}$, and were then projected onto each of the seven tomographic planes $t_1, t_2, \ldots t_7$ (Fig. 7). Reconstruction on these seven planes were made using Eq. 4, where the inverse matrices $H^{-1}_{jk}(\underline{u})$ were obtained using the point response functions $h_{ij}(\underline{r})$ expected from geometrical considerations. In these reconstructions (Fig. 8) the additive constant used was obtained by requiring that the average of the image in the outermost regions of a reconstruction was zero, since it was known a priori that there was no activity there. Some improvement is made by requiring, in these same outermost regions, that the first spatial frequency components are also zero (Fig. 9).

The difference between the results in Fig. 9 and the expected images (Fig. 6, the original octahedron summed onto the nearest reconstruction plane) is noise introduced by the reconstruction method due to random placement in a detector of the limited number of positron events from a given object source point. As expected from the smallness of the determinant near $\underline{u} = 0$, this reconstruction noise is mainly of low spatial frequency. These results show that this noise is appreciable in nuclear medicine applications. The noise is expected to be reduced when generalized inverse solutions are made for an overdetermined system and this work is in progress.

REFERENCES

1. C.A. Burnham and G.L. Brownell, A multi-Crystal Positron Camera, IEEE Trans. Nuc. Sci. NS-19, 201-205 (1972).

2. G. Muehllehner, M.P. Buchin, and J.H. Dudek, Performance Parameters of a Positron Imaging Camera, IEEE Trans. Nuc. Sci. NS-23, 528-537 (1976).

3. C.B. Lim, D. Chu, V. Perez-Mendez, L. Kaufman, R. Hattner, and D.C. Price, Initial Results of the Multiwire Proportional Chamber Positron Camera, IEEE Trans. Nuc. Sci. NS-22, 388-394 (1975).

4. G.L. Brownell, C.A. Burnham, D.A. Chesler, J.A. Correia, and B. Hoop, Transverse Section Imaging with the MGH Positron Camera, Digest of the Fourth International Conference on Medical Physics, Ottawa, Canada, July, 1976, page 14.6.

5. L.T. Chang, B. Macdonald, and V. Perez-Mendez, Axial Tomography and Three Dimensional Image Reconstruction, IEEE Trans. Nuc. Sci. NS-23, 568-572 (1976).

6. M.J. Myers, Computer Processing in Longitudinal Isotope Tomography. Proceedings 4th International Conference, Information Processing in Scintigraphy, Orsay, France, July, 1975, page 343.

Work performed under the auspices of the U. S. Energy Research and Development Administration.

FIGURE CAPTIONS

Fig. 1. Response of a large-area positron camera. All events between $-\theta$ and θ are collected.

Fig. 2. Determination of the point response functions for a 3-plane system.

Fig. 3. Point response functions $h_{jj}(\underline{r})$ measured for the U.C.S.F. positron camera. Point source in plane 1, 7 mm bins, plane separation 25 mm.

Fig. 4. First row- Tomograms made by computer simulation, with no statistical variation, of a five plane object (5mm bins, 15 mm plane separation, $\pm 45^{\circ}$ maximum data angles).
Second row- Reconstruction of these tomograms.

Fig. 5. Octahedron object composed of 33 planes of positron activity (½ cm separation, ½ cm bins) with square cross-sections in horizontal planes. Activity in inner bins is ¼ that of outer bins. Reconstruction will be done on planes $t_1, t_2, \ldots t_7$.

Fig. 6 Octahedron activity averaged over the immediate neighborhood of each of the planes $t_1, t_2, \ldots t_7$ of Fig. 5.

Fig. 7. Tomographic images resulting from two million positron events projected onto each of the planes $t_1, t_2, \ldots t_7$.

Fig. 8 Reconstruction of the tomograms of Fig. 7.

Fig. 9 Reconstruction with least squares fit to zero of the first spatial frequency components in the outer areas of the planes.

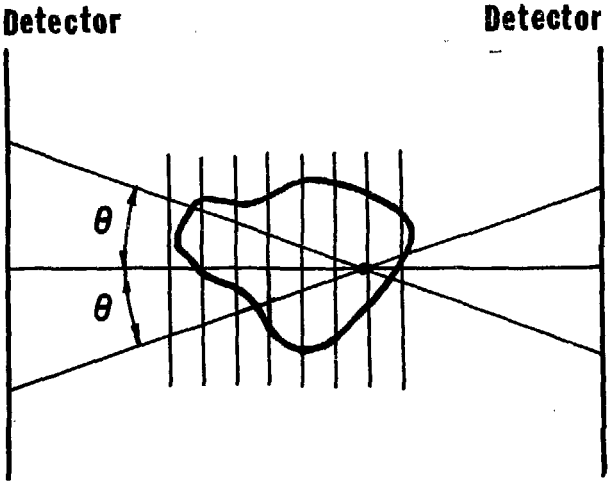

XBL 767-8844

Fig. 1

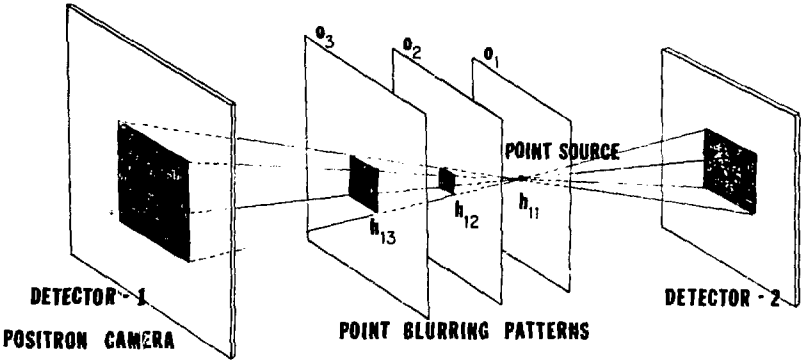
o_3
o_2
o_1
POINT SOURCE
h_{13}
h_{12}
h_{11}
DETECTOR - 1
POSITRON CAMERA
POINT BLURRING PATTERNS
DETECTOR - 2

Fig. 2

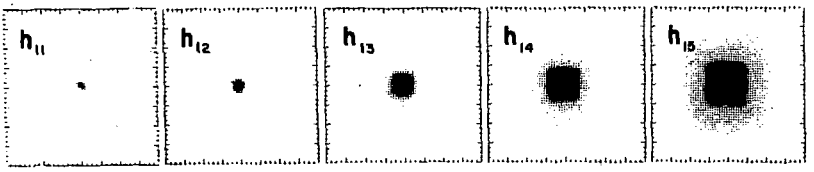

XBL 763-821

Fig. 3

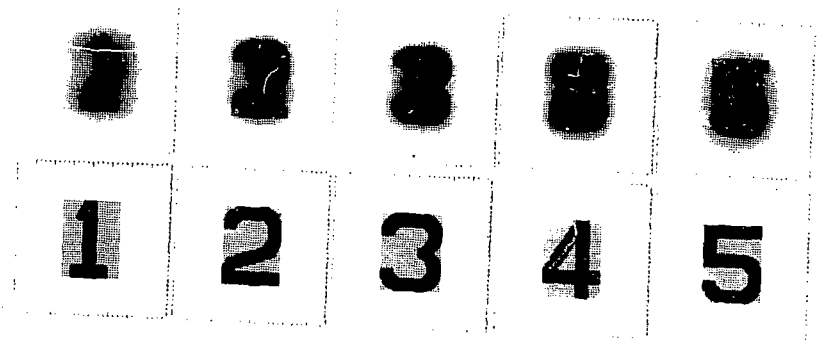

XBL 763-885

Fig. 4

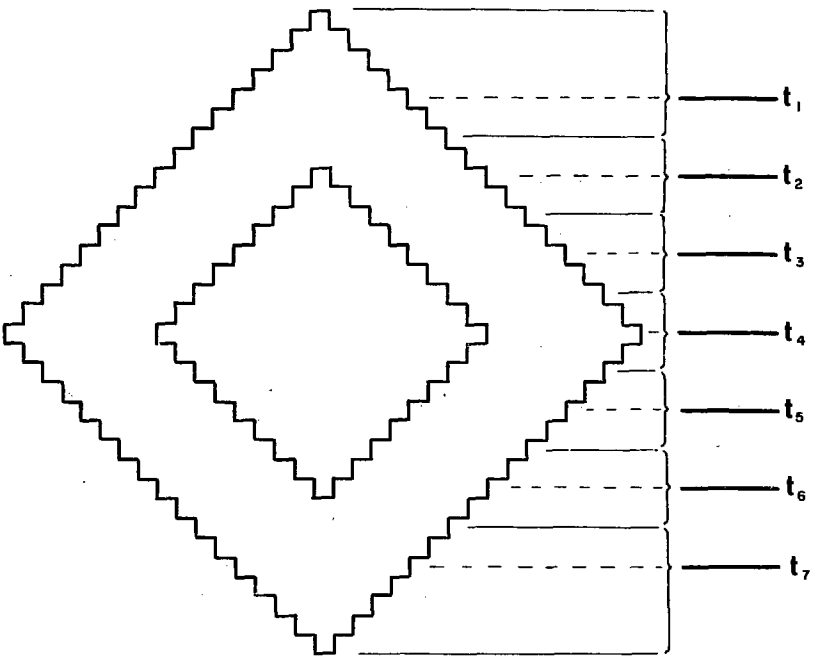

XBL 776-9136

Fig. 5

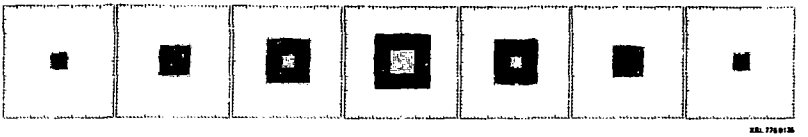

Fig. 6

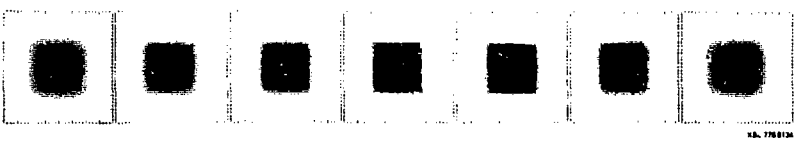

Fig. 7

XBL 786-8133

Fig. 8

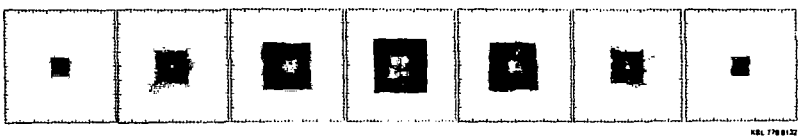

Fig. 9